Measurement-free code-switching for low overhead quantum computation using permutation invariant codes

Yingkai Ouyang,[1,*] Yumang Jing,[2] and Gavin K. Brennen[2]

[1]School of Mathematical and Physical Sciences, University of Sheffield, Sheffield, S3 7RH, United Kingdom
[2]Center for Engineered Quantum Systems, Dept. of Physics & Astronomy, Macquarie University, 2109 NSW, Australia

Transversal gates on quantum error correction codes have been a promising approach for fault-tolerant quantum computing, but are limited by the Eastin-Knill no-go theorem. Existing solutions like gate teleportation and magic state distillation are resource-intensive. We present a measurement-free code-switching protocol for universal quantum computation, switching between a stabiliser code for transversal Cliffords and a permutation-invariant code for transversal non-Cliffords that are logical Z rotations for any rational multiple of π. The novel non-Clifford gates enabled by this code-switching protocol enable implementation of a universal gate set more efficient than the Clifford+T gate set. To achieve this, we present a protocol for performing controlled-NOTs between the codes using near-term quantum control operations that employ a catalytic bosonic mode.

I. INTRODUCTION

Transversal gates [1] on quantum error correction (QEC) codes are the cornerstone of many promising approaches to realising a fault-tolerant quantum computer [2]. Transversal gates have an elegant structure which makes them fault-tolerant since they act on groups of physical qubits in parallel, thus avoiding a catastrophic spread of single errors within a code block. While using transversal gates for fault-tolerant quantum computation is attractive, for any given QEC code, the Eastin-Knill no-go theorem [1] forbids a universal set of transversal gates.

In light of the Eastin-Knill no-go theorem, the path towards realising fault-tolerant logical non-Clifford gates cannot rely on a single QEC code that implements universal quantum gates transversally. Instead, we need alternative methods. One such approach is gate teleportation [3, 4], which consumes magic states. To ensure fault tolerance, the magic states must have sufficiently high quality, achieved by distilling cleaner magic states from a larger quantity of noisy ones [5–11]. However, the magic state distillation procedure can be costly both in terms of computation time and the number of qubits used [12–14].

Code-switching [15–18] presents a conceptually simple alternative to gate-teleportation using distilled magic states for enabling universal fault-tolerant quantum computations. In code-switching, different quantum error correction codes are employed for logical Clifford and non-Clifford gates, which allows all these logical gates to be performed transversally. While code-switching offers a straightforward approach to achieve universal quantum gates fault-tolerantly, it can incur significant measurement overhead [13]. For instance, in code-switching between two stabiliser codes [19–22], one performs multiple fault-tolerant stabiliser measurements to transform one stabiliser code into another, and the number of these measurements increases with the number of errors that the stabiliser codes can correct. Another solution, amenable to surface codes, achieves a fault tolerant CCZ gate using local transversal gates and code deformations over a time that scales with the size of the qubit array [23].

A recent approach to measurement-free code-switching uses multi-qubit non-Clifford gates that are not transversal [24]. While elegant, compiling such non-transversal non-Clifford gates via near-term high-fidelity quantum control operations can be a challenge. Hence, there remains the question regarding the possibility of measurement-free code-switching using only transversal gates.

In our paper, we show how to perform high fidelity quantum computing with a universal gate set using a measurement-free code-switching protocol. In our protocol, we switch between QEC codes that encode a single logical qubit: a stabiliser code performs transversal logical Clifford gates and a permutation-invariant (PI) code that performs transversal logical non-Clifford gates. The types of such transversal non-Clifford gates include logical Z rotations for any rational multiple of π. The novel transversal non-Clifford gates that we introduce allow the implementation of gates in the binary icosahedral group and also an approximate τ_{60} gate [25] to allow the implementation of the most efficient known single-qubit universal gate set [26].

At the core of our proposed code-switching algorithm is (1) a measurement-free state-teleportation protocol and that uses only logical CNOT gates, or equivalent gate set, between a stabiliser code and a PI code and (2) our compilation of controlled-NOT gates that act between a stabiliser code and a PI code in terms of near-term quantum control. The requirements of our protocol are modest. First, we need strong, linear, coupling between the spins and the mode. In the case of coupling to a quantized cavity mode such as an optical or microwave cavity mode, this translates into the requirement for high co-operativity. Second, we require that the stabiliser code admits transversal implementations of logical Clifford gates. Third, the stabiliser code should be an *even-odd quantum code* meaning its logical zero (one) codeword can be written as a superposition of even(odd)-weight computational basis states. That is, we can write the logical zero as $|0_L\rangle = \sum_{\mathbf{x}\in\{0,1\}^n,|\mathbf{x}| \text{ even}} a_{\mathbf{x}}|\mathbf{x}\rangle$ and

* y.ouyang@sheffield.ac.uk

the logical one as $|1_L\rangle = \sum_{\mathbf{x}\in\{0,1\}^n,|\mathbf{x}| \text{ odd}} b_{\mathbf{x}}|\mathbf{x}\rangle$ for some complex coefficients $a_{\mathbf{x}}, b_{\mathbf{x}}$. As explained below, stabiliser codes with the second two properties include 2D-color codes with even stabiliser weights and an odd number of qubits [2, 27] such as the Steane code [28], and also Bacon-Shor codes [29–31] that are concatenations of odd length repetition codes. Most of the PI codes we consider here will also satisfy the even-odd code property, though we show that it is possible to switch from an even-odd stabilizer code to a non even-odd PI code using a non-linear, dispersive coupling to a mode.

II. CODE SWITCHING VIA SWAPPING

A. Transversal gates on PI codes

PI codes [32–37] allow QEC to be done on quantum states that are invariant under any permutation of the underlying particles. PI codes are attractive for various reasons. First their controllability by global fields could allow for their scalable physical implementations [38] in near-term devices such as trapped ions or ultracold atoms where addressability is challenging due to cross-talk. Second, PI codes can correct deletions, i.e. erasures at unknown locations [39, 40], along with insertion errors [41–43], which conventional QEC codes cannot correct.

The potential to implement PI codes for applications such as quantum sensing [40, 44] and quantum storage [45] has been explored. However, it was only recently recognised that PI codes can also enable the transversal implementation of logical non-Clifford gates [46, 47]. For simplicity, we first focus on two PI codes both of which encode a single logical qubit and have distance three, one on 7 qubits [46, 47], and another on 11 qubits [46]. Both of these codes lie within the family of PI codes recently introduced by Aydin et al. [47]. For a definition see Appendix A.

Permutation invariant quantum states on N qubits are superpositions of the Dicke states $|D_w^N\rangle = \binom{N}{w}^{-1/2} \sum_{x_1,\ldots,x_N\in\{0,1\}, x_1+\cdots+x_N=w} |x_1,\ldots,x_N\rangle$, of weights $w = 0,\ldots,N$. The Dicke states span the $N+1$ dimensional maximum spin ($J = N/2$) angular momentum space of the qubits. The 7-qubit PI code that we consider has support on four Dicke states [47, Example 4] and is a multi-spin analog of the Gross code on a single spin [48, Eq. (14)]. This 7-qubit code has logical codewords

$$\begin{aligned} |0_{\text{pi7}}\rangle &:= \sqrt{3/10}|D_0^7\rangle + \sqrt{7/10}|D_5^7\rangle \\ |1_{\text{pi7}}\rangle &:= \sqrt{7/10}|D_2^7\rangle - \sqrt{3/10}|D_7^7\rangle, \end{aligned} \tag{1}$$

and has distance three, but note that since the logical code words are superpositions of Dicke states with different parity weights, this is not an even-odd code. An 11-qubit PI code with distance three that was introduced in Ref [46] has logical codewords given by

$$|0_{\text{pi11}}\rangle = \frac{1}{4}(\sqrt{5}|D_0^{11}\rangle + \sqrt{11}|D_8^{11}\rangle) \tag{2}$$

$$|1_{\text{pi11}}\rangle = \frac{1}{4}(\sqrt{11}|D_3^{11}\rangle + \sqrt{5}|D_{11}^{11}\rangle). \tag{3}$$

This Kubischta-Teixeira PI code supports a transversal implementation of the logical $T = Z(\pi/4)$ gate, where $Z(\theta) := |0\rangle\langle 0| + |1\rangle\langle 1|e^{i\theta}$ denotes a qubit rotation operator about the Z-axis.

We denote a logical $Z(\theta)$ gate as $\bar{Z}_\Gamma(\theta)$ to denote a code logical operator on a set of physical qubits defined by a subsystem Γ that has the following action on the codespace spanned by logical codewords $|0_\Gamma\rangle$ and $|1_\Gamma\rangle$:

$$\bar{Z}_\Gamma(\theta)(c_0|0_\Gamma\rangle + c_1|1_\Gamma\rangle) = c_0|0_\Gamma\rangle + c_1 e^{i\theta}|1_\Gamma\rangle. \tag{4}$$

Here, we mostly use A to denote a subsystem that uses a stabiliser code, and B to denote a subsystem that uses a PI code, but in general, we only require the codes in subsystems A and B to be even-odd codes. The 7-qubit PI code admits a logical non-Clifford gate $\bar{Z}_B(4\pi/5) = Z(2\pi/5)^{\otimes 7}$ that is transversal.

Now let us denote the transversal operators on subsystem Γ as $\bar{X}_\Gamma := X^{\otimes|\Gamma|}$, $\bar{Y}_\Gamma := Y^{\otimes|\Gamma|}$, and $\bar{Z}_\Gamma := Z^{\otimes|\Gamma|}$, where X, Y, Z denote qubit Pauli matrices and $|\Gamma|$ is the number of qubits in Γ. Since $\bar{Z}_B\bar{X}_B|0_{\text{pi7}}\rangle = |1_{\text{pi7}}\rangle$ and $\bar{Z}_B\bar{X}_B|1_{\text{pi7}}\rangle = -|0_{\text{pi7}}\rangle$, the logical $-iY$ operator on the 7-qubit PI code is $X_{\text{pi7}} := \bar{Z}_B\bar{X}_B = -i\bar{Y}_B$.

The Pollatsek-Ruskai code is another 7-qubit PI code of distance three which is distinct from the 7-qubit code in (1), since it is an even-odd code [33]. The Pollatsek-Ruskai 7-qubit PI code admits transversal gates in the group 2I, the binary icosahedral group with order $|2\text{I}| = 120$ [49]. For this code, the transversal X and transversal Z operators are also the logical X and Z operators, and the transversal F gate is also the logical F gate, where $F = HZ(-\pi/2)$ and H denotes the Hadamard operator. Together, the logical X, logical Z and logical F gates generate the algebra of a binary icosahedral group 2I. Combined with the τ_{60} gate given by

$$\tau_{60} := \frac{1}{\sqrt{5\varphi+7}} \begin{pmatrix} 2+\varphi & 1-i \\ 1+i & -2-\varphi \end{pmatrix} \tag{5}$$

where $\varphi := (1+\sqrt{5})/2$, this allows us to obtain the most efficient known universal single-qubit gate set [49], providing a factor of ~ 5.9 complexity saving as compared to the usual Clifford + T gate set [50].

Turning our attention to the 11-qubit PI code, we see that $\bar{X}_B$ and $\bar{Z}_B$ implement the logical X and logical Z operators respectively. Application of the transversal T gate gives us a non-Clifford logical gate $\bar{Z}_B(3\pi/4) = T^{\otimes 11}$. Thus, we can obtain a logical T gate by applying $Z^{\otimes 11}(T^\dagger)^{\otimes 11}$. Hence we can obtain a logical T gate by applying $Z(3\pi/4)^{\otimes 11}$.

There are also PI codes that can implement logical Z rotations using transversal gates with different angles. These

codes have logical codewords

$$|0_{b,g}\rangle := (\sqrt{2b-g}|D_0^{2b+g}\rangle) + \sqrt{2b+g}|D_{2b}^{2b+g}\rangle))/\sqrt{4b},$$
$$|1_{b,g}\rangle := (\sqrt{2b-g}|D_{2b+g}^{2b+g}\rangle + \sqrt{2b+g}|D_g^{2b+g}\rangle))/\sqrt{4b}, \quad (6)$$

where g is a positive integer and $2b \geq g+1$. We call such a code a (b,g)-PI code. In Appendix B, we show that is a special case of the Aydin et al. code [47] that corrects t errors if $g \geq 2t+1$ and $2b \geq 2t+g+1$, for instance when $g = 2t+1$ and $b \geq 2t+1$. For this code, the transversal gate $Z(\pi/b)^{\otimes n}$ applies a logical Z-rotation with angle $\pi g/b$ as shown in Appendix C.

When $g = 3$, the (b,g)-PI code is equal to the Kubischta-Teixeira PI code on $2b+3$ qubits and with distance 3 [46]. Hence we can think of the (b,g)-PI code as a generalization of the $(2b+3)$-qubit Kubischta-Teixeira PI code. Note that the $(4,3)$-PI code is the 11-qubit PI code. When $b = 2^{r-1}$ for $r \geq 3$, the Kubischta-Teixeira PI code allows one to implement a logical gate in the r-th level of the Clifford hierarchy using transversal gates.

B. Even-odd quantum codes

Many PI codes are even-odd quantum codes. Indeed for g odd, the family of (b,g)-PI codes introduced above and the family of (g,n,u)-PI codes described in Ref. [34] are even-odd quantum codes. We now show that many stabilizer codes share this property as well. Bacon-Shor codes [29–31] that are concatenations of odd length codes are even-odd quantum codes. The logical zero and one of a repetition code are $|0\rangle^{\otimes n}$ and $|1\rangle^{\otimes n}$ respectively, which have even and odd weight computational basis states for odd n. Moreover, in the Hadamard basis, the logical zero and one also are superpositions of only even and odd weight computational basis states for odd n. Since the concatenation of an even-odd quantum code with an even-odd quantum code results in an even-odd quantum code, the Bacon-Shor codes that are the concatenation of odd length repetition codes in the standard basis and the Hadamard basis must also be even-odd quantum codes.

The 2D-color codes with even stabiliser weights and an odd number of qubits are also even-odd quantum codes. Such codes have stabilisers generated by Paulis operators with only X-type stabilisers and Z-type stabilisers, and admit transversal Clifford gates as their logical gates. Note that we can write the logical zero of such a code to be proportional to the state $\sum_{P\in S} P|0\rangle^{\otimes n}$, where S denotes the stabiliser of the code. The X-type generators have even weights, which implies that the logical zero operator must be a superposition over even weight computational basis states. Since the transversal X gate is the logical X gate which takes the logical zero state to the logical one state and there is an odd number of qubits, the logical one state must be a superposition over odd weight computational basis states. Hence such 2D-color codes are even-odd quantum codes.

C. High-level code-switching protocol

One measurement-free approach to swap two qubits is to apply three controlled-NOT (CNOT) gates. The following circuit shows how to swap a pair of qubits with two CNOT gates if one of the states is known [4, Eq (1)]:

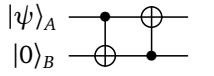

(7)

For our code-switching protocol, we treat system A as the stabiliser code on $|A|$ qubits, and system B as a PI code on $|B|$ qubits. Based on (7), we can write the logical variant of the swap circuit using two CNOT gates and a known PI ancilla prepared in the $|0_B\rangle$. Using this idea, starting from a stabiliser code where we can perform logical Clifford gates transversally, we switch to a PI code to perform a logical non-Clifford gate transversally before switching back to the stabiliser code. We can achieve this using the following protocol:

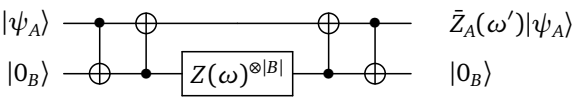

Using the 11-qubit PI code, we can obtain the logical T gate on the stabiliser code with $\omega = 3\pi/4$ and $\omega' = \pi/4$. Using the 7-qubit PI code, we can obtain a logical non-Clifford on the stabiliser code with $\omega = 2\pi/5$ and $\omega' = 4\pi/5$.

Since both of these codes have distance equal to 3, they both allow the correction of any single-qubit error on the logical information.

We can code-switch to PI codes with larger distance, and which admit transversal implementation of other exotic non-Clifford gates. Now let g and b be coprime so that there exists an integer k such that $\text{mod}(kg, b) = 1$. Then the (b,g)-PI code on $(2b+g)$ qubits can implement the logical $Z(\pi u/b)$ gate transversally on the stabiliser code with $\omega = uk\pi/b$ for any integer u, while allowing the correction of $\lfloor(\min\{g, 2b-g\}-1)/2\rfloor$ errors. For example, using an $11a$-qubit $(4a,3a)$-PI code, we can obtain a logical T on the stabiliser code with $\omega = 3\pi/4$ that corrects $\lfloor(3a-1)/2\rfloor$ errors. When $r \geq 2$, the $(2^r a, 3a)$-PI code on $(2^r+3)a$ qubits allows us to obtain the logical $Z(\pi/2^r)$ gate transversally with $\omega = k\pi/2^r a$ and $\text{mod}(3k, 2^r) = 1$ while correcting $\lfloor(3a-1)/2\rfloor$ errors.

III. GEOMETRIC PHASE GATES

Our proposed mechanism to process quantum information in PI codes uses geometric phase gates (GPGs) arising from coupling quantum spins to a coherently controllable bosonic mode [51, 52]. This flavor of GPG is a standard tool for entangling gates in trapped ion quantum processors [53], where the bosonic mode is a quantized motional mode. Other suitable architectures, as outlined in Ref. [54], include trapped atoms in optical cavities [55], superconducting qubits coupled via a driven microwave resonator

[56], or polar molecules coupled to microwave stripline cavities [57].

To understand the action of the gate, consider the spin operator $\hat{w}_\Gamma = \frac{|\Gamma|}{2}\mathbf{1} - \hat{J}^z_\Gamma$ that counts the Hamming weight of spin states, where $\hat{J}^z_\Gamma = \frac{1}{2}\sum_{j=1}^{|\Gamma|} Z_{\Gamma,j}$ is the collective angular momentum operator. Here, $Z_{\Gamma,j}$ applies a phase flip on the jth qubit of system Γ and applies the identity operator on all other qubits of Γ. We describe three types of GPGs here. The first two use an interaction between the spins in Γ and the mode that is linear in the creation and annihilation operators of the mode, while the third other uses a dispersive interaction that is quadratic in bosonic operators:

$$U = \begin{cases} e^{i\phi\hat{w}^2_\Gamma} & \text{Linear GPG-A [51]} \\ e^{-iI/(\delta-\hat{w}_\Gamma g^2/\Delta)} & \text{Linear GPG-B [54]} \\ e^{-i2\chi\sin(\theta\hat{w}_\Gamma+\beta)} & \text{Non-linear GPG [58]} \end{cases} \tag{8}$$

In the Linear GPG-A gate, also known as the Mølmer-Sørensen gate, the angle $\phi \in [0, 2\pi)$ is fully tunable through the control pulses used in the implementation. Recently it has been shown using optimal control methods that this gate together with global rotations of the spins provides for efficient exactly universal state and unitary synthesis in the Dicke state space [59–61]. In the Linear GPG-B gate introduced in Ref. [54] the relevant parameters are intensity I, and the detunings δ, Δ which are tunable within a range whereas the coupling strength g between the spins and cavity is usually treated as constant. This gate enables a broader class of entangling gates like the multi-controlled phase gate $C_{N-1}(Z)$. For the non-linear GPG, the angles $\chi, \theta, \beta \in [0, 2\pi)$ are fully controllable through a combination of dispersive interaction evolutions punctuated by displacement operations on the mode. Complemented by global spin rotations this gate is also exactly universal for state and unitary synthesis in the Dicke space [38].

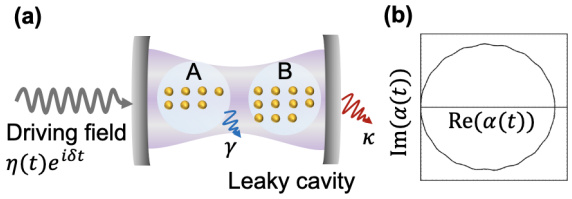

FIG. 1. (a) Two registers of qubits are coupled to a common cavity mode with strength g. The cavity mode decays at a rate κ, while the spins decay from their excited state states at a rate γ. The cavity acts as a mediator of interactions between the qubits, allowing the two registers to influence one another through their coupling to the same cavity mode. (b) Illustration of a closed trajectory in phase space of a coherent state $\alpha(t)$ of the cavity mode associated to an eigenspace of the spin operator $\hat{w}_\Gamma$ for a Linear GPG. After the gate, the mode and the spins are disentangled and the phase accumulated on the eigenspace depends on the area of the trajectory.

IV. PI ANCILLA STATE PREPARATION

Logical state preparation of a target PI state $|\Psi_t\rangle$ can be achieved using the linear GPG-A gate, which we simply denote (l-GPG) [60, 61]. Starting in the product state $|D^N_0\rangle$, one applies a sequence of gates:

$$|\Psi\rangle = \prod_{p=1}^{P}[R(\theta_p, \xi_p, \gamma_p)U(\phi_p)]|D^N_0\rangle \tag{9}$$

that prepares an output approximating $|\Psi_t\rangle$, where P denotes the number of pulses. The GPGs $U(\phi_p)$ are interleaved with global rotations around an arbitrary axis as

$$\begin{aligned} R(\theta_p, \xi_p, \gamma_p) &= R_z(\theta_p)R_y(\xi_p)R_z(\gamma_p) \\ &= e^{i\theta_p\hat{J}^z}e^{i\xi_p\hat{J}^y}e^{i\gamma_p\hat{J}^z}. \end{aligned} \tag{10}$$

The parameters θ_p, ξ_p, γ_p and ϕ_p are chosen numerically to minimize the infidelity $1 - |\langle\Psi|\Psi_t\rangle|^2$. Here, for simplicity, instead of using the definition of the l-GPG above with $U(\phi) = e^{i\phi\hat{w}^2_\Gamma}$, we exploit the decomposition

$$e^{i\phi_p\hat{w}^2_\Gamma} = e^{i\phi_p(\frac{|\Gamma|^2}{4} - |\Gamma|\hat{J}^z_\Gamma + \hat{J}^{z^2}_\Gamma)}, \tag{11}$$

and instead define $U(\phi_p) = e^{i\phi_p\hat{J}^{z^2}_\Gamma}$, since the constant and the $\hat{J}^z_\Gamma$ term in the exponent can be absorbed into the global rotation R during the optimization. This allows us to treat the contribution by evolution generated by $\hat{J}^z_\Gamma$ as part of a uniform rotation without affecting the overall dynamics of the system.

We now discuss the state preparation using l-GPGs in the presence of errors. We assume that the rotations are noise-free, as they can typically be performed fast relative to the spin mode coupling g. We apply the error model presented in Ref. [54] in the presence of losses from cavity mode decay at rate κ and the spontaneous emission of the spin excited state at rate γ. In the Dicke subspace, the ideal pth l-GPG $U(\phi_p)$ is modified to the erroneous mapping as

$$\mathcal{E}(\phi_p, \rho_{p-1}) = \sum_{n,m=0}^{N} \langle D^N_n|\rho_{p-1}|D^N_m\rangle f_{n,m}(\phi_p)|D^N_n\rangle\langle D^N_m|, \tag{12}$$

where

$$f_{n,m}(\phi_p) = e^{-(m-n)^2\frac{|\phi_p|}{2}\sqrt{\frac{2(1+2^{-N})}{C}} - (m+n)\frac{|\phi_p|}{2}\frac{1}{\sqrt{2C(1+2^{-N})}}}e^{-i(n^2-m^2)\phi_p} \tag{13}$$

and $C = g^2/\kappa\gamma$ is the cooperativity of the cavity supporting the mode. Here, we apply the absolute value on the parameter ϕ_p as it can take negative values during numerical optimization.

The full preparation is a concatenation of erroneous GPGs $\mathcal{E}(\phi_p, \rho_{p-1})$ interleaved with error-free rotations $R(\theta_p, \xi_p, \gamma_p)$, which is written as,

$$\mathcal{E}_{\text{l-GPG}} = \mathcal{E}^P_{\text{l-GPG}} \circ \mathcal{E}^{P-1}_{\text{l-GPG}} \circ \cdots \circ \mathcal{E}^1_{\text{l-GPG}}, \tag{14}$$

where $\mathcal{E}^{p}_{\text{l-GPG}} = R(\theta_p, \xi_p, \gamma_p)\mathcal{E}(\phi_p, \rho_{p-1})R^{\dagger}(\theta_p, \xi_p, \gamma_p)$. We apply Eq. (14) to the initial state $\rho_0 = |D_0^N\rangle\langle D_0^N|$ and use infidelity $1 - \langle\Psi_t|\rho_P|\Psi_t\rangle$ as the cost function, where ρ_P is the output state after P number of pulses are applied, and $|\Psi_t\rangle$ is the target state. In our optimization, we fix the total number of pulses P and utilize MATLAB's built-in toolbox, which employs the Sequential Quadratic Programming (SQP) method, to minimize the cost function and obtain lists of parameters θ_p, ξ_p, γ_p and ϕ_p. It should be noted that the optimization method applied is non-deterministic.

V. IMPLEMENTING ENTANGLING LOGICAL GATES

The different GPG's discussed above enable different logical operations to be used for code switching. The non-linear GPG can implement logical CNOT gates between a non even-odd PI code, like the PI-7 code, and an even-odd stabilizer code (see Appendix E). However, the dispersive interactions between the spins and the cavity mode necessary to instantiate the non-linear GPG are less directly accessible in physical systems [38], and the dispersive interaction strengths tend to be smaller than linear interaction strengths implying slower gates. We therefore focus most of our analysis on using linear GPGs.

A. Using linear GPGs with the PI-11 code

Instead of the switching circuit shown in Sec. II C, we discuss a variation of it, with the idea that logical CZ gates are easier to be implemented than CNOTs. In what follows we show how to implement the following circuit for code switching between the Steane code (system A) and the 11-qubit PI code (system B):

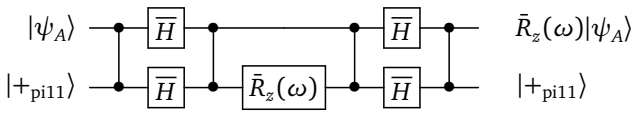

1. *Implementing the* $C_{A(B)}Z_{B(A)}$ *gate*

To realize the CZ, which acts symmetrically on the control and target, it suffices to construct a gate that up to global phase on the logical subspace, applies a minus sign on the logical basis state $|1\rangle_A|1\rangle_B$ and acts trivially on the other logical basis states. When both A and B are even-odd quantum codes, as is the case here, then we have the following decomposition in terms of three l-GPGs

$$\text{CZ} = e^{i\frac{\pi}{2}\hat{w}^2_{A\cup B}} e^{-i\frac{\pi}{2}\hat{w}^2_{A}} e^{-i\frac{\pi}{2}\hat{w}^2_{B}}. \tag{15}$$

Here an l-GPG involving the operator $\hat{w}_{A\cup B} = \hat{w}_A + \hat{w}_B$ can be obtained by coupling all the spins constituting codes A and B to the same bosonic mode. The process infidelity for performing each of the three l-GPGs in this sequence is [54]

$$1 - F = \frac{\pi|\Gamma|}{2\sqrt{2(1+2^{-|\Gamma|})C}}. \tag{16}$$

.

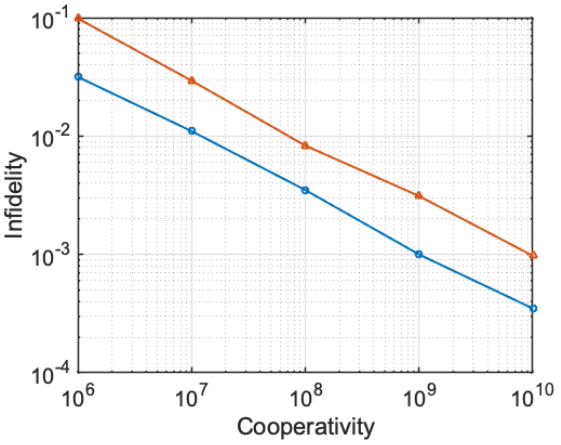

FIG. 2. Process infidelity $1-F_{\text{pro}}(\mathcal{E}_{\overline{H}}, \overline{\mathcal{H}})$ for implementing the logical Hadamard gate (orange, triangles), and state infidelity $1 - \langle+_{\text{pi11}}|\rho|+_{\text{pi11}}\rangle$ for preparing the logical $|+_{\text{pi11}}\rangle$ state (blue,circles), using GPGs as a function of cooperativity C. In both cases $P = 10$ gate sequences are used for the state preparation steps.

2. *Implementing the logical* $\overline{\text{H}}$ *gate*

Next, we discuss a way to implement a logical Hadamard gate $\overline{H}$ for the PI-11 code. In the code space, the eigenvalues of $\overline{H}$ are ±1 with corresponding eigenstates:

$$|\lambda_+\rangle = \frac{1}{\sqrt{2(2+\sqrt{2})}}[(1+\sqrt{2})|0_{\text{pi11}}\rangle + |1_{\text{pi11}}\rangle],$$
$$|\lambda_-\rangle = \frac{1}{\sqrt{2(2-\sqrt{2})}}[(1-\sqrt{2})|0_{\text{pi11}}\rangle + |1_{\text{pi11}}\rangle]. \tag{17}$$

We can use the method of PI state preparation to construct a unitary on the entire Dicke space which acts correctly in the logical subspace. Using the spectral decomposition, $\overline{H}$ must have the form,

$$\overline{H} = |\lambda_+\rangle\langle\lambda_+| - |\lambda_-\rangle\langle\lambda_-| + \sum_s e^{i\beta_s}|\beta_s\rangle\langle\beta_s|, \tag{18}$$

here $\{|\beta_s\rangle\}$ are any set of orthonormal vectors which are contained completely in the ortho-complement to the code space, and $\{\beta_s\}$ are any eigenvalues of on those states. We can construct this gate with linear GPGs using the method of state preparations adapted for subspaces [62]. Specifically we can write

$$\overline{H} = We^{i\pi|D_N^N\rangle\langle D_N^N|}W^{\dagger} \tag{19}$$

where W is any unitary extension of the state preparation: $W|D_N^N\rangle = |\lambda_-\rangle$. The diagonal phase gate $e^{i\pi|D_N^N\rangle\langle D_N^N|}$ is the $C_{N-1}(Z)$ gate, where $N = 11$ for the PI-11 code. This gate can be synthesized from linear GPG-B gates using the methods in Ref. [54].

We characterize the performance of the implemented Hadamard gate described by Eq. (19) in the presence of losses using the fidelity-based measure $F_{\text{pro}}(\mathcal{E}_{\overline{H}}, \overline{\mathcal{H}})$ proposed in Ref. [63] to compare the performance of actual realized process $\mathcal{E}_{\overline{H}}$ against the ideal unitary process $\overline{\mathcal{H}}(\rho) = \overline{H}_{\text{ide}}\rho\overline{H}_{\text{ide}}^\dagger$, where $\overline{H}_{\text{ide}}$ is the ideal Hadamard gate in logical subspace. The actual process for the implementation of logical Hadamard gate is given by

$$\mathcal{E}_{\overline{H}} = \mathcal{E}_{\text{l-GPG}} \circ \mathcal{E}_{\text{ph}} \circ \mathcal{E}^{\text{R}}_{\text{l-GPG}}, \tag{20}$$

where $\mathcal{E}_{\text{ph}}(\rho) = F_{\text{ph}} C_{N-1}(Z)\rho C_{N-1}^\dagger(Z)$ is the erroneous map of the middle phase gate in Eq. (19). $\mathcal{E}_{\text{l-GPG}}$ ($\mathcal{E}^{\text{R}}_{\text{l-GPG}}$) is the (reverse of) preparation mapping associated with W ($W^\dagger$) in the presence of losses, as detailed in Eq. (14). Here, for simplicity, we optimize parameters solely for the preparation process and apply the same parameters to the reverse mapping without additional optimization. The fidelity measure $F_{\text{pro}}(\mathcal{E}_{\overline{H}}, \overline{\mathcal{H}})$ is computed based on process matrices, which necessitates the superoperator formalism for each mapping in Eq. (20). The detailed calculations are provided in Appendix D.

In Fig. 2, we plot the infidelity for: the implementation error of the Hadamard gate (orange), and the preparation error (blue) for the PI-11 code as a function of the cooperativity C. The simulation is performed in the presence of loss errors as described in Eq. (12). Following the approximation in Ref. [54] (Eq. (25)), the infidelity of the $\overline{H}$ implementation can be estimated as $1 - F_{\text{pro}}(\mathcal{E}_{\overline{H}}, \overline{\mathcal{H}}) \sim 21.78 \times N/\sqrt{C}$, where we consider 18 non-trivial GPG operations for the preparation step and its inverse, with $\theta = \pi/2$. The infidelity for the middle $C_{N-1}(Z)$ gate is approximated by $1.8 \times N/\sqrt{C}$. Similarly, the infidelity for state preparation is estimated by $1 - \langle +_{\text{pi11}}|\rho|+_{\text{pi11}}\rangle \sim 9.99 \times N/\sqrt{C}$, where 9 non-trivial GPG gates are considered, again with $\theta = \pi/2$. Our simulation results indicate a somewhat better performance with the infidelity scaling as $1 - F_{\text{pro}}(\mathcal{E}_{\overline{H}}, \overline{\mathcal{H}}) \sim 8.29 \times N/C^{0.4985}$ and $1 - \langle +_{\text{pi11}}|\rho|+_{\text{pi11}}\rangle \sim 2.80 \times N/C^{0.4953}$, indicating lower infidelity compared to the approximation.

VI. APPROXIMATION OF THE SUPER GOLDEN GATE

The most efficient single-qubit gate set is given by representations of the binary icosahedral group $2I$ (which can be implemented with the Pollatsek-Ruskai code) and the super golden gate τ_{60} given in (5). Here we give an approximate decomposition of τ_{60} which can be achieved by code-switching between bg-PI codes, the Pollatsek-Ruskai code that implements 2I, and PI codes that implement the transversal T gate.

Let $S = Z(\pi/2)$, and $T = Z(\pi/4)$. Let H denote the Hadamard gate, and Z denote $Z(\pi)$. Noting that the super golden gate squares to the identity, we can write it in an Euler decomposition as

$$\tau_{60} = e^{-i\frac{\pi}{8}Z} e^{-i\theta Y} e^{-i\frac{3\pi}{8}Z},$$

where $\theta = \cos^{-1}\frac{2+\varphi}{\sqrt{5\varphi+7}}$. We can further simplify

$$\begin{aligned} \tau_{60} &= Te^{-i\theta Y}ZT^\dagger \\ &= TSHe^{-i\theta Z}HS^\dagger ZT^\dagger. \end{aligned}$$

Now θ/π can be approximated by a rational. Defining

$$\begin{aligned} \tilde{\tau}_{60}(\gamma) &= TSHR_Z(\gamma)HS^\dagger ZT^\dagger \\ &= TF^\dagger R_Z(\gamma)FZT^\dagger \end{aligned}$$

we find $\|\tilde{\tau}_{60}(\gamma) - \tau_{60}\|_F < 1.88 \times 10^{-6}$ for $\gamma = \frac{\pi 334}{1408}$, where $\|\cdot\|_F$ denotes the Frobenius norm. This could be achieved using: a $(1408, 334)$—PI code for the small angle Z rotation, a smaller (b, g)—PI code for transversal T gates, and a PI code like the Pollatsek-Ruskai code admitting transversal gates in the group 2I (noting $F^2 = F^\dagger$ up to a global phase).

VII. CONCLUSION

We have presented a method for code switching between a stabilizer code and a permutation invariant code, and along the way have introduced a family of PI codes with a tunable set of transversal, non-Clifford gates. It is noteworthy that our measurement-free code-switching scheme is also applicable to transitions between two stabiliser codes, provided they satisfy the even-odd quantum code structure. In comparison to the measurement-based approach, our scheme eliminates the overhead associated with measurements and reduces the gate operation complexity by utilising collective gate implementations. We leave an analysis of to what extent our method can be made fault tolerant to future work.

VIII. ACKNOWLEDGEMENTS

Y.O. acknowledges support from EPSRC (Grant No. EP/W028115/1). G.K.B. and Y.J. acknowledge support from the Australian Research Council Centre of Excellence for Engineered Quantum Systems (Grant No. CE 170100009).

[1] B. Eastin and E. Knill, Restrictions on transversal encoded quantum gate sets, Phys. Rev. Lett. **102**, 110502 (2009).

[2] E. T. Campbell, B. M. Terhal, and C. Vuillot, Roads towards fault-tolerant universal quantum computation, Nature **549**,

172 EP (2017).
[3] D. Gottesman and I. L. Chuang, Demonstrating the viability of universal quantum computation using teleportation and single-qubit operations, Nature **402**, 390 (1999).
[4] X. Zhou, D. W. Leung, and I. L. Chuang, Methodology for quantum logic gate construction, Physical Review A **62**, 052316 (2000).
[5] S. Bravyi and A. Kitaev, Universal quantum computation with ideal clifford gates and noisy ancillas, Physical Review A **71**, 022316 (2005).
[6] S. Bravyi and J. Haah, Magic-state distillation with low overhead, Phys. Rev. A **86**, 052329 (2012).
[7] A. Krishna and J.-P. Tillich, Towards low overhead magic state distillation, Phys. Rev. Lett. **123**, 070507 (2019).
[8] E. T. Campbell and M. Howard, Unified framework for magic state distillation and multiqubit gate synthesis with reduced resource cost, Phys. Rev. A **95**, 022316 (2017).
[9] E. T. Campbell and M. Howard, Unifying gate synthesis and magic state distillation, Phys. Rev. Lett. **118**, 060501 (2017).
[10] B. Eastin, Distilling one-qubit magic states into toffoli states, Phys. Rev. A **87**, 032321 (2013).
[11] M. B. Hastings and J. Haah, Distillation with sublogarithmic overhead, Phys. Rev. Lett. **120**, 050504 (2018).
[12] J. O'Gorman and E. T. Campbell, Quantum computation with realistic magic-state factories, Phys. Rev. A **95**, 032338 (2017).
[13] M. E. Beverland, A. Kubica, and K. M. Svore, Cost of universality: A comparative study of the overhead of state distillation and code switching with color codes, PRX Quantum **2**, 020341 (2021).
[14] D. Litinski, Magic State Distillation: Not as Costly as You Think, Quantum **3**, 205 (2019).
[15] J. T. Anderson, G. Duclos-Cianci, and D. Poulin, Fault-tolerant conversion between the steane and reed-muller quantum codes, Phys. Rev. Lett. **113**, 080501 (2014).
[16] H. Bombín, Dimensional jump in quantum error correction, New Journal of Physics **18**, 043038 (2016).
[17] A. Kubica and M. E. Beverland, Universal transversal gates with color codes: A simplified approach, Phys. Rev. A **91**, 032330 (2015).
[18] H. Poulsen Nautrup, N. Friis, and H. J. Briegel, Fault-tolerant interface between quantum memories and quantum processors, Nature communications **8**, 1321 (2017).
[19] S. Heußen and J. Hilder, Efficient fault-tolerant code switching via one-way transversal cnot gates, arXiv preprint arXiv:2409.13465 (2024).
[20] F. Butt, S. Heußen, M. Rispler, and M. Müller, Fault-tolerant code-switching protocols for near-term quantum processors, PRX Quantum **5**, 020345 (2024).
[21] I. Pogorelov, F. Butt, L. Postler, C. D. Marciniak, P. Schindler, M. Müller, and T. Monz, Experimental fault-tolerant code switching, arXiv preprint arXiv:2403.13732 (2024).
[22] J. Huang, S. M. Li, L. Yeh, A. Kissinger, M. Mosca, and M. Vasmer, Graphical CSS code transformation using ZX calculus, arXiv preprint arXiv:2307.02437 (2023).
[23] B. J. Brown, A fault-tolerant non-clifford gate for the surface code in two dimensions, Science Advances **6**, eaay4929 (2020), https://www.science.org/doi/pdf/10.1126/sciadv.aay4929.
[24] S. Heußen, D. F. Locher, and M. Müller, Measurement-free fault-tolerant quantum error correction in near-term devices, PRX Quantum **5**, 010333 (2024).
[25] E. Kubischta and I. Teixeira, Family of quantum codes with exotic transversal gates, Physical Review Letters **131**, 240601 (2023).
[26] O. Parzanchevski and P. Sarnak, Super-golden-gates for pu(2), Advances in Mathematics **327**, 869 (2018), special volume honoring David Kazhdan.
[27] H. Bombín, Gauge color codes: optimal transversal gates and gauge fixing in topological stabilizer codes, New Journal of Physics **17**, 083002 (2015).
[28] A. M. Steane, Error correcting codes in quantum theory, Phys. Rev. Lett. **77**, 793 (1996).
[29] P. W. Shor, Scheme for reducing decoherence in quantum computer memory, Phys. Rev. A **52**, R2493 (1995).
[30] D. Bacon, Operator quantum error-correcting subsystems for self-correcting quantum memories, Phys. Rev. A **73**, 012340 (2006).
[31] P. Aliferis and A. W. Cross, Subsystem fault tolerance with the bacon-shor code, Phys. Rev. Lett. **98**, 220502 (2007).
[32] M. B. Ruskai, Pauli Exchange Errors in Quantum Computation, Physical Review Letters **85**, 194 (2000).
[33] H. Pollatsek and M. B. Ruskai, Permutationally invariant codes for quantum error correction, Linear Algebra and its Applications **392**, 255 (2004).
[34] Y. Ouyang, Permutation-invariant quantum codes, Physical Review A **90**, 062317 (2014), 1302.3247.
[35] Y. Ouyang and J. Fitzsimons, Permutation-invariant codes encoding more than one qubit, Physical Review A **93**, 042340 (2016).
[36] Y. Ouyang, Permutation-invariant qudit codes from polynomials, Linear Algebra and its Applications **532**, 43 (2017).
[37] R. Movassagh and Y. Ouyang, Constructing quantum codes from any classical code and their embedding in ground space of local hamiltonians, arXiv preprint arXiv:2012.01453 10.48550/arXiv.2012.01453 (2020).
[38] M. T. Johnsson, N. R. Mukty, D. Burgarth, T. Volz, and G. K. Brennen, Geometric pathway to scalable quantum sensing, Phys. Rev. Lett. **125**, 190403 (2020).
[39] Y. Ouyang, Permutation-invariant quantum coding for quantum deletion channels, in *2021 IEEE International Symposium on Information Theory (ISIT)* (2021) pp. 1499–1503.
[40] Y. Ouyang and G. K. Brennen, Finite round quantum error correction on symmetric quantum sensors (2023), arXiv:2212.06285 [quant-ph].
[41] M. Hagiwara, The four qubits deletion code is the first quantum insertion code, IEICE Communications Express **10**, 243 (2021).
[42] T. Shibayama and Y. Ouyang, The equivalence between correctability of deletions and insertions of separable states in quantum codes, in *2021 IEEE Information Theory Workshop (ITW)* (IEEE, 2021) pp. 1–6.
[43] T. Shibayama and M. Hagiwara, Equivalence of quantum single insertion and single deletion error-correctabilities, and construction of codes and decoders, in *2022 IEEE International Symposium on Information Theory (ISIT)* (IEEE, 2022) pp. 2957–2962.
[44] Y. Ouyang, N. Shettell, and D. Markham, Robust quantum metrology with explicit symmetric states, IEEE Transactions on Information Theory **68**, 1809 (2022).
[45] Y. Ouyang, Quantum storage in quantum ferromagnets, Phys. Rev. B **103**, 144417 (2021).
[46] E. Kubischta and I. Teixeira, The not-so-secret fourth parameter of quantum codes, arXiv preprint arXiv:2310.17652 10.48550/arXiv.2310.17652 (2023).
[47] A. Aydin, M. A. Alekseyev, and A. Barg, A family of permutationally invariant quantum codes, Quantum **8**, 1321 (2024).

[48] J. A. Gross, Designing codes around interactions: The case of a spin, Phys. Rev. Lett. **127**, 010504 (2021).

[49] E. Kubischta and I. Teixeira, Family of quantum codes with exotic transversal gates, Phys. Rev. Lett. **131**, 240601 (2023).

[50] P. O. Boykin, T. Mor, M. Pulver, V. Roychowdhury, and F. Vatan, On universal and fault-tolerant quantum computing: a novel basis and a new constructive proof of universality for Shor's basis, in *Foundations of Computer Science, 1999. 40th Annual Symposium on* (1999) pp. 486–494.

[51] K. Mølmer and A. Sørensen, Multiparticle Entanglement of Hot Trapped Ions, Physical Review Letters **82**, 1835 (1999).

[52] A. Luis, Quantum mechanics as a geometric phase: phase-space interferometers, Journal of Physics A: Mathematical and General **34**, 7677 (2001).

[53] D. Leibfried, B. DeMarco, V. Meyer, D. Lucas, M. Barrett, J. Britton, W. M. Itano, B. Jelenković, C. Langer, T. Rosenband, and D. J. Wineland, Experimental demonstration of a robust, high-fidelity geometric two ion-qubit phase gate, Nature **422**, 412 (2003).

[54] S. Jandura, V. Srivastava, L. Pecorari, G. Brennen, and G. Pupillo, Non-local multi-qubit quantum gates via a driven cavity (2023), arXiv:2303.13127 [quant-ph].

[55] A. S. Sørensen and K. Mølmer, Measurement induced entanglement and quantum computation with atoms in optical cavities, Phys. Rev. Lett. **91**, 097905 (2003).

[56] L. B. Nguyen, Y.-H. Lin, A. Somoroff, R. Mencia, N. Grabon, and V. E. Manucharyan, High-coherence fluxonium qubit, Phys. Rev. X **9**, 041041 (2019).

[57] A. André, D. DeMille, J. M. Doyle, M. D. Lukin, S. E. Maxwell, P. Rabl, R. J. Schoelkopf, and P. Zoller, A coherent all-electrical interface between polar molecules and mesoscopic superconducting resonators, Nature Physics **2**, 636 (2006).

[58] X. Wang and P. Zanardi, Simulation of many-body interactions by conditional geometric phases, Phys. Rev. A **65**, 032327 (2002).

[59] N. Gutman, A. Gorlach, O. Tziperman, R. Ruimy, and I. Kaminer, Universal control of symmetric states using spin squeezing, Phys. Rev. Lett. **132**, 153601 (2024).

[60] L. J. Bond, M. J. Davis, J. Minář, R. Gerritsma, G. K. Brennen, and A. Safavi-Naini, Efficient state preparation for metrology and quantum error correction with global control, arXiv preprint arXiv:2312.05060 10.48550/arXiv.2312.05060 (2023).

[61] V. Srivastava, S. Jandura, G. K. Brennen, and G. Pupillo, Entanglement-enhanced quantum sensing via optimal global control (2024), arXiv:2409.12932 [quant-ph].

[62] G. K. Brennen, D. P. O'Leary, and S. S. Bullock, Criteria for exact qudit universality, Phys. Rev. A **71**, 052318 (2005).

[63] A. Gilchrist, N. K. Langford, and M. A. Nielsen, Distance measures to compare real and ideal quantum processes, Physical Review A—Atomic, Molecular, and Optical Physics **71**, 062310 (2005).

Appendix A: AAB+ code

The AAB+ type code is specified by three integer parameters g, m and δ, with logical codewords given by

$$|0_{(g,m,\delta,+)}\rangle = \sum_{l \text{ even}} \gamma b_l |D^n_{gl}\rangle + \sum_{l \text{ odd}} \gamma b_l |D^n_{n-gl}\rangle, \tag{A1}$$

$$|1_{(g,m,\delta,+)}\rangle = \sum_{l \text{ even}} \gamma b_l |D^n_{n-gl}\rangle + \sum_{l \text{ odd}} \gamma b_l |D^n_{gl}\rangle, \tag{A2}$$

where $b_l = \sqrt{\binom{m}{l}/\binom{n/g-l}{m+1}}$ and $\gamma = \sqrt{\binom{n/(2g)}{m}\frac{n-2gm}{g(m+1)}}$, and $n = 2gm+\delta+1$. The code corrects t errors when $g \geq 2t+1$, $m \geq t$ and $\delta \geq 2t$.

In Appendix B, we show that the (b,g)-PI code is the $(g, 1, 2b-g-1)$ AAB+ code. From the property of the AAB+ code, the (b,g)-PI code corrects t errors if $g \geq 2t+1$ and $2b-g-1 \geq 2t$.

Next we turn our attention to the transversal non-Clifford gate. We consider the gate $T_b = Z(\pi/b)$. Then we see that

$$T_b^{\otimes n}|0_{b,g}\rangle = |0_{b,g}\rangle, \tag{A3}$$

$$T_b^{\otimes n}|1_{b,g}\rangle = e^{ig\pi/b}|0_{b,g}\rangle. \tag{A4}$$

From this, we see that the transversal gate $T_b^{\otimes n}$ gate applies a logical Z-rotation with angle $\pi g/b$.

Appendix B: Proof that the (b,g)-PI code is an AAB+ code

To have the (b,g)-PI code, the parameter m in the AAB+ type code must be equal to 1, because each logical codeword is a superposition of two Dicke states. By setting $m=1$, we have

$$b_0 = 1/\sqrt{\binom{n/g}{2}} = g/\sqrt{n(n-g)/2}, \tag{B1}$$

$$b_1 = 1/\sqrt{\binom{n/g-1}{2}} = g/\sqrt{(n-g)(n-2g)/2}, \tag{B2}$$

$$\gamma = \sqrt{\frac{n}{2g}\frac{\delta+1}{2g}} = \sqrt{n(\delta+1)}/(2g). \tag{B3}$$

Then we have

$$\gamma b_0 = \sqrt{n(\delta+1)}/\sqrt{2n(n-g)} = \sqrt{\frac{\delta+1}{2(n-g)}}, \tag{B4}$$

$$\gamma b_1 = \sqrt{n(\delta+1)}/\sqrt{2(n-g)(n-2g)} = \sqrt{\frac{n(\delta+1)}{2(n-g)(n-2g)}}. \tag{B5}$$

Now consider having $n = 2b+g$ for some positive integer b so that $\delta = 2b-g-1$, $n-g = 2b, n-2g = 2b-g$. Then

$$\gamma b_0 = \sqrt{\frac{2b-g}{4b}} = \sqrt{\frac{1}{2} - \frac{g}{4b}}, \tag{B6}$$

$$\gamma b_1 = \sqrt{\frac{n(2b-g)}{4b(2b-g)}} = \sqrt{\frac{2b+g}{4b}} = \sqrt{\frac{1}{2} + \frac{g}{4b}}. \tag{B7}$$

This shows that the (b,g)-PI codes are just $(g,1,2b-g-1)$-AAB+ codes. The condition for (b,g)-PI codes to correct t errors is that $g \geq 2t+1$ and that $2b-g-1 \geq 2t$. The second condition is equivalent to $2b \geq g+2t+1$.

When $g=3, m=1, \delta = 2^r - 4$, the AAB+ code can implement the logical gate for $T^{2^{3-r}}$ transversally for $r \geq 3$ [47].

Appendix C: Transversal non-Clifford logical operations on (b,g)-PI codes

Our code supports transversal X as the logical X. If n is odd (which is when g is odd), then the transversal Z is the logical Z. If n is even (when g is even), the transversal Z gate stabilizes the code.

Whenever b and g are coprime, we can implement the logical $\pi k/b$ rotation transversally for any $k = 0,\ldots,b-1$. For the (b,g)-PI code to correct t errors, it suffices to have $b \geq \frac{g+1}{2} + t$ and $g \geq 2t+1$. When b and g are coprime, we can implement a logical T_b^k gate transversally for any $k = 0,\ldots,b-1$ by setting g as the smallest coprime number to a fixed b.

The $(4a,3a)$-PI code on $n = 11a$ qubits admits $(T_4^9)^{\otimes n}$ as the logical T gate, and corrects $\lfloor (3a-1)/2 \rfloor$ errors. Proof: We will also find transversal T codes analytically of higher distances. For this we choose $g/b = 3/4$. This allows the logical T gate by applying the $\pi 3/4$ gate thrice. Hence $b = 4g/3$ needs to be an integer. We choose g to be a multiple of 3. That is $g = 3a$ for some positive integer a. Then $b = 4a$. Then for the corresponding AAB+ code, we have $\delta = 2b-g-1 = 8a-3a-1 = 5a-1$. So the condition on δ we need is $5a-1 \geq t$ which is $5a \geq t+1$. This is trivially satisfied from the condition on g given by $3a \geq 2t+1$. Hence the codes that implement the transversal T have length $8a+3a = 11a$, and correct $\lfloor (3a-1)/2 \rfloor$ errors. These codes have shorter lengths than those discussed by Kubischta and Teixeira [46]. For example to correct two errors, Kubischta and Teixeira [46] find a 27 qubit PI code. For 3 errors, Kubischta and Teixeira [46] find a 49 qubit code. Here, $a = 1,2,3$ correspond to an 11-qubit code, 22 qubit code and 33 qubit code that correct 1,2, and 4 errors respectively.

When $r \geq 2$, the $(2^r a, 3a)$-PI code on $(2^r+3)a$ qubits implements the logical T_{2^r} gate transversally, and corrects $\lfloor (3a-1)/2 \rfloor$ errors. Proof: We can also find codes for transversal gates in the Clifford hierarchy. For this we choose $g/b = 3/2^r$ for $r \geq 2$. Then we need $b = 2^r g/3$ to be an integer, and hence choose g to be a multiple of 3. That is $g = 3a$ for some positive integer a and $b = 2^r a$. This allows the logical T gate by applying the $\pi 3/2^r$ gate an integer number of times, because there exists an integer k such that $3k = 1 \mod 2^r$. This is because 3 and 2^r are coprime. Now we check the distance condition. $\delta = 2b-g-1 = 2^{r+1}a - 3a - 1 = (2^{r+1}-3)a - 1$. So the condition on δ is $2^{r+1}a - 3a \geq 2t+1$. But when $r \geq 2$, this condition trivially holds when $3a \geq 2t+1$. Hence the codes have length $2^{r+1}a + 3a$ and correct $\lfloor (3a-1)/2 \rfloor$ errors. When $r=3$, $a = 1,2,3$ correspond to an 19-qubit code, 38 qubit code and 57 qubit code that correct $1,2$ and 4 errors respectively and can implement a transversal $\sqrt{T}$ gate. When $r=4$, $a = 1,2,3$ correspond to an 35-qubit code, 70 qubit code and 105 qubit code that correct $1,2$ and 4 errors respectively and can implement a transversal $T^{1/4}$ gate.

Appendix D: Fidelity measure for Hadamard gate process

In this section, we discuss how to evaluate the fidelity measure using process matrices. The process matrix gives a convenient way of describing the evolution of quantum states, especially when dealing with mixed states or open quantum systems where the state is described by a density matrix. In the case of a unitary operation $\rho' = U\rho U^\dagger$, if we vectorize the density matrix ρ using the row-stacking operation, the action of the superoperator can be expressed in a matrix form as

$$|\rho'\rangle\rangle = \mathcal{U}|\rho\rangle\rangle, \tag{D1}$$

where $\mathcal{U} = U \otimes U^*$. U^* is the complex conjugate of U and $\otimes$ denotes the Kronecker product.

In our case, for the preparation mapping described in Eq. (14), the global rotations R are unitary and their associated superoperators are represented in the Kronecker product form. Though the erroneous GPG mapping in Eq.(12) is non-unitary, it does not induce coherence between different state components, and can thus be constructed as a diagonal matrix in the superoperator formalism. Consequently, the superoperator associated with the preparation mapping $\mathcal{E}_{\text{l-GPG}}$ is given by

$$E_{\text{l-GPG}} = \prod_{p=P}^{1} [R(\theta_p,\xi_p,\gamma_p) \otimes R^*(\theta_p,\xi_p,\gamma_p)] \mathcal{G}_p(\phi_p), \tag{D2}$$

where $\mathcal{G}_p(\phi_p)$ is a $(N+1)^2 \times (N+1)^2$ diagonal matrix that has elements

$$\langle D_n^N | \langle D_m^N | \mathcal{G}_p(\phi_p) | D_n^N \rangle | D_m^N \rangle = f_{n,m}(\phi_p) \tag{D3}$$

on each diagonal position accordingly.

Analogously, the superoperator associated with the reverse mapping of the preparation $\mathcal{E}^{\text{R}}_{\text{l-GPG}}$ is given by

$$E^{\text{R}}_{\text{l-GPG}} = \prod_{p=1}^{P} \mathcal{G}_p(-\phi_p) [R^\dagger(\theta_p,\xi_p,\gamma_p) \otimes (R^\dagger(\theta_p,\xi_p,\gamma_p))^*]. \tag{D4}$$

The middle phase gate in Eq. (19) is unitary but has an overall fidelity factor F_{ph}. We express its superoperator as

$$E_{\text{ph}} = F_{\text{ph}} C_{N-1}(Z) \otimes C^*_{N-1}(Z). \tag{D5}$$

Thus, the actual mapping for the implementation of the logical Hadamard gate in the superoperator formalism is given by

$$E = E_{\mathrm{l-GPG}} E_{\mathrm{ph}} E^{\mathrm{R}}_{\mathrm{l-GPG}}. \tag{D6}$$

Since our primary concern is whether the implemented Hadamard gate acts correctly in the logical subspace, we project E from the Dicke subspace onto the logical $\{|0_{\mathrm{L}}\rangle, |1_{\mathrm{L}}\rangle\}$ subspace, resulting in

$$E_{\mathrm{L}} = \begin{pmatrix} E_{00,00} & E_{00,01} & E_{00,10} & E_{00,11} \\ E_{01,00} & E_{01,01} & E_{01,10} & E_{01,11} \\ E_{10,00} & E_{10,01} & E_{10,10} & E_{10,11} \\ E_{11,00} & E_{11,01} & E_{11,10} & E_{11,11} \end{pmatrix}, \tag{D7}$$

where $E_{x'y',xy} = \langle x'_{\mathrm{L}}|\langle y'_{\mathrm{L}}|E|x_{\mathrm{L}}\rangle|y_{\mathrm{L}}\rangle$. Following the method in Ref. [63], the process fidelity between $\mathcal{E}_{\overline{H}}$ and $\overline{\mathcal{H}}$ can be simply calculated as

$$F_{\mathrm{pro}}(\mathcal{E}_{\overline{H}}, \overline{\mathcal{H}}) = \frac{1}{8}\sum_j \mathrm{Tr}[\overline{H}_{\mathrm{ide}} U_j^\dagger \overline{H}_{\mathrm{ide}} \mathcal{E}_{\overline{H}}(U_j)], \tag{D8}$$

where $\{U_j\}$ are orthonormal bases of unitary operators. Here, in the logical subspace, we select $U_0 = I_2, U_1 = X, U_2 = Y, U_3 = Z$ (where I_2, X, Y and Z are the identity and Pauli matrices). Substitution into Eq. (D8) gives

$$\begin{aligned} F_{\mathrm{pro}}(\mathcal{E}_{\overline{H}}, \overline{\mathcal{H}}) &= \frac{1}{8}(\mathrm{Tr}[\mathcal{E}_{\overline{H}}(I_2)] + \mathrm{Tr}[Z\mathcal{E}_{\overline{H}}(X)] + \mathrm{Tr}[-Y\mathcal{E}_{\overline{H}}(Y)] + \mathrm{Tr}[X\mathcal{E}_{\overline{H}}(Z)]) \\ &= \frac{1}{8}\left[\begin{pmatrix} 1 & 0 & 0 & 1 \end{pmatrix} E_{\mathrm{L}} \begin{pmatrix} 1 \\ 0 \\ 0 \\ 1 \end{pmatrix} + \begin{pmatrix} 1 & 0 & 0 & -1 \end{pmatrix} E_{\mathrm{L}} \begin{pmatrix} 0 \\ 1 \\ 1 \\ 0 \end{pmatrix} + \begin{pmatrix} 0 & i & -i & 0 \end{pmatrix} E_{\mathrm{L}} \begin{pmatrix} 0 \\ -i \\ i \\ 0 \end{pmatrix} + \begin{pmatrix} 0 & 1 & 1 & 0 \end{pmatrix} E_{\mathrm{L}} \begin{pmatrix} 1 \\ 0 \\ 0 \\ -1 \end{pmatrix} \right] \\ &= \frac{1}{8}(E_{00,00} + E_{00,11} + E_{11,00} + E_{11,11} + E_{00,01} + E_{00,10} - E_{11,01} - E_{11,10} \\ &\quad - E_{01,01} + E_{01,10} + E_{10,01} - E_{10,10} + E_{01,00} - E_{01,11} + E_{10,00} - E_{10,11}) \end{aligned} \tag{D9}$$

Appendix E: Non-linear GPGs for switching between an even-odd code and a non even-odd code

In this section we describe how to directly implement code switching using logical CNOT gates which works even when the PI code is not an even-odd code, as is the case for the PI-7 code. This requires use of non-linear GPGs and to explain the mechanism we first review how this highly non-linear spin gate is implemented from elementary interactions.

1. Implementing the non-linear GPG

The dispersive interaction between spins and the bosonic mode we consider takes the form $H = g\hat{a}^\dagger\hat{a} \otimes \hat{w}_\Gamma$. Evolving the dispersive interaction H for a time t generates the operator $R(\theta\hat{w}_\Gamma) := e^{i\theta\hat{w}_\Gamma \otimes \hat{a}^\dagger\hat{a}}$ where $\theta = gt$. This applies a rotation in phase space by an amount proportional to the eigenvalues associated to eigenspaces of the Hermitian operator $\hat{w}$ acting on subsystem Γ. Note it is possible to generate $R(-\theta\hat{w}_\Gamma)$ by reversing the coupling strength $g \to -g$ which can be done in some physical setups by e.g. changing the sign of detuning of the cavity mode from the spin transition frequency.

Under conjugation by rotations, displacements can be made conditional on the spin states:

$$D(\alpha e^{i\theta\hat{w}_\Gamma}) = R(\theta\hat{w}_\Gamma) D(\alpha) R(-\theta\hat{w}_\Gamma). \tag{E1}$$

We can similarly make mode rotations conditional on the spin states using the operator

$$\Lambda_\Gamma(\alpha, \theta) := D(\alpha) R(\theta\hat{w}_\Gamma) D(-\alpha) R(-\theta\hat{w}_\Gamma). \tag{E2}$$

A composition of displacement and conditional displacement operators around a closed trajectory in phase space, provides for an identity operator on the mode and a geometric phase gate on the spins:

$$\begin{aligned} U_{\mathrm{GPG}}(\theta, \phi, \chi) &= D(-\beta) R(\theta\hat{w}_\Gamma) D(-\alpha) R(-\theta\hat{w}_\Gamma) \\ &\quad \times D(\beta) R(\theta\hat{w}_\Gamma) D(\alpha) R(-\theta\hat{w}_\Gamma) \\ &= e^{-i2\chi\sin(\theta\hat{w}_\Gamma + \phi)}. \end{aligned}$$

$\phi = \arg(\alpha) - \arg(\beta)$. If the mode begins as the vacuum state then the first rotation operator is not needed.

a. *Implementing the* $\mathrm{C}_B\mathrm{X}_A$ *gate*

First, consider the gate $\mathrm{C_BX_A}$ which has the PI code as control and a stabiliser code as target. The stabiliser code

is assumed to be an even-odd code, while The PI code has its logical zero codeword $|0_B\rangle$ and logical one codeword $|1_B\rangle$ consisting of superpositions of states with Hamming weight 0 mod q and s mod q respectively. In the case of the PI-7 code, $q=5$ and $s=2$.

Here, we construct a controlled geometric phase gate that traverses a path in phase space with zero area if the control has weight 0 mod q, while producing the area required to generate a transversal X gate on the target if the control has s mod q.

If we pick $\gamma = s\pi/q$, then the action of the controlled displacement operator $\Lambda_B(\alpha, s\pi/q)$ on the codespace of the PI code is

$$\begin{aligned}&\Lambda_B(\alpha,s\pi/q)(c_0|0_B\rangle + c_1|1_B\rangle)\otimes|\psi_{\text{mode}}\rangle\\ =&c_0|0_B\rangle\otimes|\psi_{\text{mode}}\rangle + c_1|1_B\rangle\otimes D(\alpha(1-e^{2is\pi/q}))|\psi_{\text{mode}}\rangle.\end{aligned} \tag{E3}$$

We can use these controlled displacements between the PI code and the mode to produce a GPG on the stabiliser code conditional on the logical state of PI code:

$$\begin{aligned}\Lambda_B(U_{\text{GPG}}(\theta,\phi,\chi)) :=&\Lambda_B(-\beta,s\pi/q)R(\theta J^z_{\text{A}})\Lambda_B(-\alpha,s\pi/q)\\ &\times R(-\theta J^z_{\text{A}})\Lambda_B(\beta,s\pi/q)R(\theta J^z_{\text{A}})\\ &\times\Lambda_B(\alpha,s\pi/q)R(-\theta J^z_{\text{A}}),\end{aligned} \tag{E4}$$

where $\chi = |\alpha\beta||1-e^{2is\pi/q}|^2 = 4|\alpha\beta|\sin^2(s\pi/q)$ and $\phi = \arg(\alpha)-\arg(\beta)$. The action of this conditional GPG on the codespace of the PI code and stabiliser code is

$$\begin{aligned}&\Lambda_B(U_{\text{GPG}}(\theta,\phi,\chi))(c_0|0_B\rangle + c_1|1_B\rangle)\otimes|\psi_A\rangle\\ =&c_0|0_B\rangle\otimes|\psi_A\rangle + c_1|1_B\rangle\otimes e^{-i2\chi\sin(\theta\hat{J}^z_A+\phi)}|\psi_A\rangle.\end{aligned} \tag{E5}$$

We pick $\alpha=\beta$ so that $\phi=0$. With the choice $\theta=\pi$, when the control is in $|1_B\rangle$, the mode experiences a trajectory in phase space that is a rotated square with area χ, and when the control is in $|0_B\rangle$ the trajectory has zero area. If we further pick $\chi=\pi/4$, i.e. $\alpha=\sqrt{\pi}/(4|\sin(s\pi/q)|)$, then $e^{-i2\chi\sin(\theta\hat{J}^z_A)} = i\prod_{j=1}^7 Z_j = i\bar{Z}_A$, where $\bar{Z}_A$ is the logical Z operator on the stabiliser code.

The final gate is then

$$\text{C}_\text{B}\text{X}_\text{A} \;=\; \bar{S}_A\bar{H}_A\Lambda_1(U_{\text{GPG}}(\pi,0,\tfrac{\pi}{4}))\bar{H}_A, \tag{E6}$$

where $\bar{H}_A = H^{\otimes|A|}$ is the transversal logical Hadamard and $\bar{S}_A = \bar{Z}S^{\otimes|A|}$ is the logical $S=Z(\pi/2)$ gate on the stabiliser code.

b. *Implementing the* C_AX_B *gate*

Second, consider the gate $\text{C}_\text{A}\text{X}_\text{B}$ which has the stabiliser code as the control and the PI code as target. We can use the same procedure as in Sec. E 1 a, with the roles of A and B reversed, except we choose $g\tau=\gamma=\pi$ and for the rotation operator we use $\hat{w}_B = \hat{J}^y_B = \frac{1}{2}\sum_{j\in B}Y_j$. In this case the action angle in phase space will be $\chi = 4|\alpha|^2$ and the geometric phase gate will have the parameters $\phi=\pi$, $\theta=\pi$, and $\alpha=\beta=\sqrt{\pi}/4$. This will achieve the operation $-i\bar{Y}_B$ if the control is in $|0_A\rangle$. In summary,

$$\begin{aligned}\text{C}_\text{A}\text{X}_\text{B} \;&=\; \Lambda_A(U_{\text{GPG}}(\pi,\pi,\tfrac{\pi}{4}))\\ &=\; \Lambda_A(-\tfrac{\sqrt{\pi}}{4},\pi)R(\pi\hat{J}^y_\text{B})\Lambda_A(-\tfrac{\sqrt{\pi}}{4},\pi)\\ &\quad\times R(-\pi\hat{J}^y_\text{B})\Lambda_A(\tfrac{\sqrt{\pi}}{4},\pi)R(\pi\hat{J}^y_\text{B})\\ &\quad\times\Lambda_A(\tfrac{\sqrt{\pi}}{4},\pi)R(-\pi\hat{J}^y_\text{B}).\end{aligned} \tag{E7}$$